American Mineralogist, Volume 63, pages 47–57, 1978

Mineralogy of the Elwin Bay kimberlite, Somerset Island, N.W.T., Canada

ROGER H. MITCHELL

Department of Geology, Lakehead University
Thunder Bay, Ontario, Canada

Abstract

The Elwin Bay kimberlite is a small post-Silurian diatreme characterized by the presence of ultrabasic xenoliths and chrome-poor garnet megacrysts [Mg/(Mg+Fe) = 0.79–0.83; Cr_2O_3 = 0.12–2.3%]. Olivine [Mg/(Mg+Fe) = 0.89–0.94] occurs as large rounded "phenocrysts" and as smaller groundmass crystals. Chemically and texturally the "rounded phenocrysts" are identical to olivines found in garnet lherzolite xenoliths and as xenocrysts in this kimberlite. Phlogopite occurs as rounded phenocrysts (0.6–3.2% TiO_2) and as euhedral groundmass laths (0.2–0.8% TiO_2). The groundmass mineral assemblage is composed of calcite, monticellite (3.2–7.5% FeO), perovskite (1.3–1.6% FeO), serpentine, chlorite, and spinel. Pre-fluidization spinels are rounded Ti-poor aluminous-magnesian-chromites. Post-fluidization spinels are euhedral titaniferous-magnesian-aluminous-chromites (1.5–7.1% TiO_2). Calcite and primary serpentine-filled ocelli are considered to represent separation of a late-stage immiscible carbonate fluid.

Introduction

The Somerset Island kimberlite province has been briefly described by Mitchell (1976), and is analogous to the Southern African kimberlite province in that dikes and diatremes of kimberlite, micaceous kimberlite, and calcareous kimberlite are spatially and possibly genetically related. So far mineralogical data is available only for the Peuyuk kimberlite (Mitchell and Clarke, 1976). This paper presents the results of a study of the Elwin Bay kimberlite, which is unusual in that it contains abundant monticellite.

The Elwin Bay diatreme is a small circular intrusion (diameter *ca.* 200 m) about 1 km south of Elwin Bay at the eastern margin of Somerset Island (Fig. 1). The diatreme is emplaced in Silurian limestones and is exposed on a ridge as frost-heaved regolith, no true outcrop being present. In hand specimen the kimberlite is a black to greenish-black porphyritic rock with phenocrysts of olivine and phlogopite and megacrysts of garnet. The intrusion appears to consist of a single petrographic type of kimberlite; no multiple intrusion of the kind found at the Peuyuk diatreme is evident. The principal variations in the appearance of the kimberlite are due to variations in the amount of calcite groundmass and the amount of xenolithic material. Rounded-to-angular xenoliths are either country-rock carbonates or mantle-derived ultramafic xenoliths (Mitchell, 1977).

Compositions of minerals in the kimberlite were determined at Purdue University, using a MAC 500 automated microprobe (Finger and Hadidiacos, 1972) and the Bence and Albee (1968) correction procedure.

Olivine

Olivine occurs in two generations, an earlier generation of rounded "phenocrystal" olivines and a second generation of euhedral to subhedral post-fluidization olivines. Pre- and post-fluidization olivines are distinguished on the basis of textural criteria. All large (>1 mm) rounded olivines are considered to have crystallized prior to the fluidized intrusion of the diatreme. Fluidization is an intrusive process which results in the mechanical rounding of all preexisting phenocrysts and xenocrysts (Dawson, 1962). Euhedral small (<1 mm) olivines (groundmass olivines) not showing such abrasive effects are considered to have grown after fluidization. It is difficult to distinguish texturally between olivines that are true phenocrysts and those that were derived by the disaggregation of ultramafic xenoliths. Single olivine crystals which are strongly strained are probably de-

0003–004X/78/0102–0047$02.00

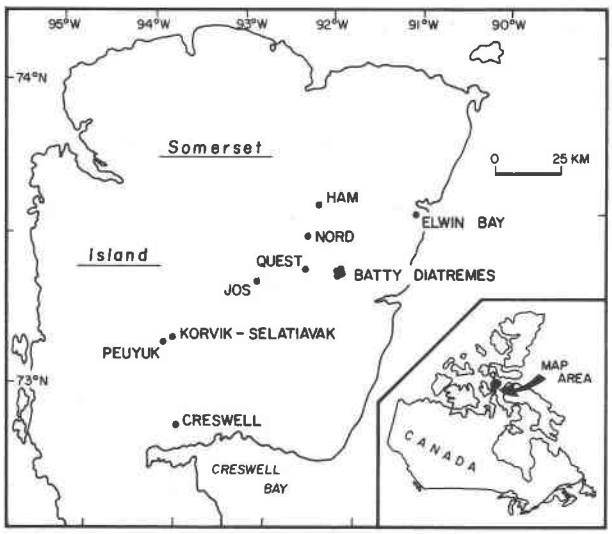

Fig. 1. The Somerset Island kimberlite province.

rived from porphyroclastic lherzolite xenoliths, but this criterion cannot be applied to olivines derived from strain-free coarse lherzolites. Figure 2 shows that pre-fluidization rounded "phenocrystal" olivines range in composition from Fo_{88}–$Fo_{93.5}$, with the majority of compositions lying between Fo_{91} and Fo_{93}. A similar range is seen in the euhedral groundmass olivines, but the majority of these olivines is richer in iron than Fo_{91}. The compositions of the "phenocrystal" olivines overlap the compositions of the olivines in the Elwin Bay ultramafic xenoliths (Mitchell, 1977), and the maxima on the histograms are coincident. Figure 2 implies that phenocrystal and xenocrystal olivines cannot be chemically distinguished from each other, but that olivines less magnesian than Fo_{91} probably crystallized from the kimberlite magma. The range in olivine composition seen at Elwin Bay is similar to that found in the Peuyuk kimberlite (Mitchell and Fritz, 1973). This latter kimberlite lacks ultramafic xenoliths, and the most magnesian (Fo_{93}) rounded phenocrystal olivines are considered to be true phenocrysts. Phenocrystal olivines of similar composition probably occur in the Elwin Bay kimberlite, but they cannot be distinguished from the xenocrystal olivines either texturally or chemically. All olivines are weakly zoned (1% Fo) towards more iron-rich margins and do not exhibit the strong NiO zonation seen in the Peuyuk olivines. Calcium contents are uniformly low (<0.2% CaO), even in groundmass olivines which have crystallized at low pressures together with calcite and monticellite. This is in agreement with Warner and Luth's (1973) data for the Mg_2SiO_4–$CaMgSiO_4$ solvus, which indicates that olivines contain less than 1 mol percent $CaMgSiO_4$ in solid solution at low temperature.

The olivines have undergone a variety of alterations, and serpentinization and chlorithization are predominant. The groundmass olivines are more susceptable to alteration than the phenocrysts. Representative analyses of serpentine and septechlorite are given in Table 1. The serpentines contain unusually high iron contents, a feature noted also by Emeleus and Andrews (1975) in the West Greenland kimberlites. Iron-bearing serpentine of this type appears to form only when iron is not expelled from the olivine as magnetite during the serpentinization process. This may be the result of serpentinization at relatively low oxygen fugacities. Serpentine and septechlorites are typically colorless, but some examples

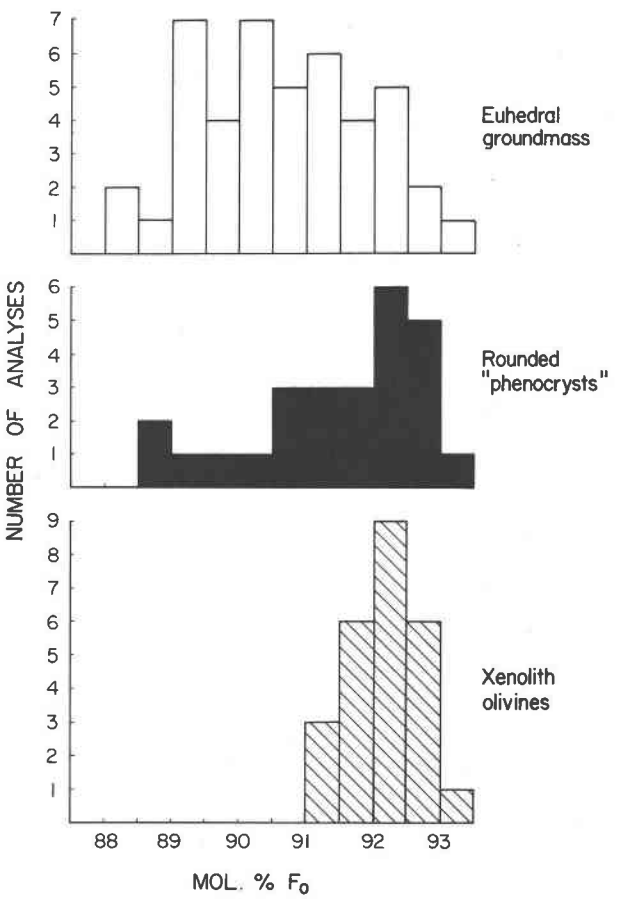

Fig. 2. Composition of phenocrystal and groundmass olivine in the Elwin Bay kimberlite compared with that of olivine in Elwin Bay lherzolite.

Table 1. Composition of serpentines from the Elwin Bay kimberlite; total Fe given as FeO

	1	2	3	4	5	6	7	8	9
SiO_2	39.61	39.96	39.24	37.41	32.15	31.96	42.10	39.98	0.37
TiO_2	0.03	0.00	0.00	0.00	0.00	0.00	0.01	0.02	0.02
Al_2O_3	0.23	0.53	0.70	0.20	0.17	0.05	0.22	0.48	0.11
Cr_2O_3	0.00	0.00	0.05	0.00	0.00	0.00	0.03	0.02	0.02
FeO	5.77	3.60	3.50	5.36	9.83	7.09	3.02	3.58	31.34
MnO	0.09	0.05	0.08	0.00	0.07	0.12	0.06	0.12	0.61
MgO	39.18	39.09	39.84	40.20	37.93	45.17	38.50	41.68	51.83
CaO	0.09	0.08	0.09	0.15	1.48	0.20	0.10	0.05	0.96
Na_2O	0.00	0.13	0.21	0.00	0.07	0.03	0.00	0.09	0.00
NiO	0.00	0.00	1.02	0.28	0.26	0.33	0.00	0.00	0.16
	85.03	83.43	84.76	83.61	81.96	84.97	84.10	85.01	85.25

1 - 2 groundmass serpentine
3 serpentine after olivine
4 blue pleochroic serpentine after olivine
5 blue pleochroic septechlorite (?)
6 colorless septechlorite after olivine
7 - 8 serpentine in calcite ocelli
9 red brucite-geothite mixture after olivine

exhibit a strong blue phleochroism of unknown origin. Other alterations of olivine include pseudomorphing by calcite and replacement by a fine-grained bright orange-red material which is probably a mixture of brucite and goethite (Table 2, analysis 9).

Garnets

Red garnets occur as large (1–2 cm) rounded megacrysts. Representative analyses are given in Table 2. Megacryst garnet compositions fall into three groups in the statistical classification of Dawson and Stephens (1975), *i.e.* groups 1, 2, and 9. Garnets in the garnet lherzolite xenoliths also fall into Dawson and Stephens' group 9, but these garnets are easily distinguished from the group 9 megacryst garnets by their purple color, higher Cr_2O_3 content (Fig. 3), and smaller size (max. 5 mm). Xenocrystal chrome-pyrope derived by the fragmentation of garnet lherzolite can be found in the kimberlite. Dawson and Stephens' present group 9 category seems not to be a useful indicator of garnet origin, since it can incorporate garnets of two different origins. Further subdivision on the basis of Cr_2O_3 should be attempted. Figure 3 shows that groups 1 and 2 garnets have higher TiO_2 contents than any of the group 9 garnets. Figure 4 illustrates the major-element variation of the garnets, and indicates that groups 1 and 2 probably form a continuum of compositions rather than two discrete groups, a conclusion also reached by Dawson and Stephens when considering garnet compositions from a single kimberlite pipe rather than all available garnet analyses. The Elwin Bay garnet megacrysts are chemically very similar to those found in the Frank Smith and Monastery kimberlites (Boyd and Dawson, 1972), the Artur de Paiva kimberlite (Boyd and Danchin, 1974), and the Sloan diatreme (Eggler and McCallum, 1974), and evidently can be regarded as a characteristic megacryst of kimberlite. Intergrowths of garnet with magnesian ilmenite, clinopyroxene, and orthopyroxene are found in the southern African occurrences. No such intergrowths have yet been found at Elwin Bay.

The larger size and chrome-poor nature of megacryst garnets relative to the smaller chrome-rich pyropes of the garnet lherzolites argue against the megacrysts being derived by the fragmentation of ultramafic xenoliths; thus an origin must be sought in the processes which give rise to kimberlite magma. Boyd and Dawson (1972) believe that the range in

Table 2. Representative analyses of garnets from the Elwin Bay kimberlite

	1	2	3	4	5	6
SiO_2	41.94	42.66	42.40	42.36	42.42	41.23
TiO_2	0.80	0.47	0.94	0.87	0.13	0.17
Al_2O_3	21.16	21.59	21.08	21.08	20.87	22.92
Cr_2O_3	1.36	1.86	1.19	1.36	2.42	1.25
FeO	7.66	6.54	8.32	7.85	8.30	8.91
MnO	0.26	0.27	0.25	0.24	0.43	0.37
MgO	21.35	22.14	20.49	21.24	19.83	21.12
CaO	5.06	4.44	5.26	5.18	5.17	4.43
Na_2O	0.15	0.09	0.10	0.08	0.09	0.04
	99.75	100.03	100.04	100.26	99.66	100.44
Structural Formula based on 12 oxygens.						
Si	2.993	3.012	3.022	3.008	3.043	2.932
Al	1.780	1.797	1.711	1.765	1.764	1.921
Ti	0.043	0.025	0.050	0.047	0.007	0.009
Cr	0.077	0.104	0.067	0.076	0.137	0.070
Fe	0.457	0.386	0.496	0.466	0.498	0.530
Mn	0.016	0.016	0.015	0.014	0.026	0.022
Mg	2.271	2.330	2.177	2.248	2.120	2.239
Ca	0.387	0.336	0.402	0.394	0.397	0.338
Na	0.021	0.012	0.014	0.011	0.013	0.006
Mg/Mg+Fe	0.83	0.86	0.81	0.83	0.81	0.81

1 - 2 Group 1 garnets
3 - 4 Group 2 garnets
5 - 6 Group 9 low Cr_2O_3 garnets

Mg/(Mg+Fe) ratios of the megacrysts reflects an igneous differentiation event, but are unable to determine whether this took place in the low-velocity zone prior to kimberlite formation (Boyd and Nixon 1975) or as a part of the process of kimberlite formation. In the former case the megacrysts would be xenocrysts, in the latter phenocrysts. I favor the latter case, the garnets being a liquidus phase at high pressure in kimberlite magma (Mitchell and Clarke, 1976), a hypothesis also advocated by Dawson and Stephens (1975).

Mica

Phlogopite occurs in two generations, as rounded pale brown phenocrysts which are commonly broken and kink-banded, and as very pale yellow, euhedral, deformation-free groundmass laths. Representative analyses are presented in Table 3. Analysis of the phlogopite was difficult because of the pervasive chloritization of all samples. Phenocrystal micas are richer in TiO_2 than groundmass mica, and are similar in composition to phlogopite phenocrysts from the Peuyuk diatreme (Clarke and Mitchell, 1975). Dawson and Smith (1975) consider that megacryst phlogopites of similar composition from South African kimberlites are true phenocrysts and are not derived by the fragmentation of phlogopite-bearing lherzolites. The Elwin Bay groundmass euhedral phlogopite crystallized directly from the kimberlite magma. Phlogopite similar in composition to this groundmass phlogopite is also formed during metasomatism of the country-rock xenoliths in this diatreme.

Spinels

Textural relationships indicate that three parageneses of spinel are present in this kimberlite.

(1) Prefluidization, transparent aluminous-magnesian-chromites, which have been rounded and abraded during fluidization.

(2) Opaque Al_2O_3-poor titaniferous-magnesian-chromite that occurs as mantles upon prefluidization spinels and as discrete euhedral crystals.

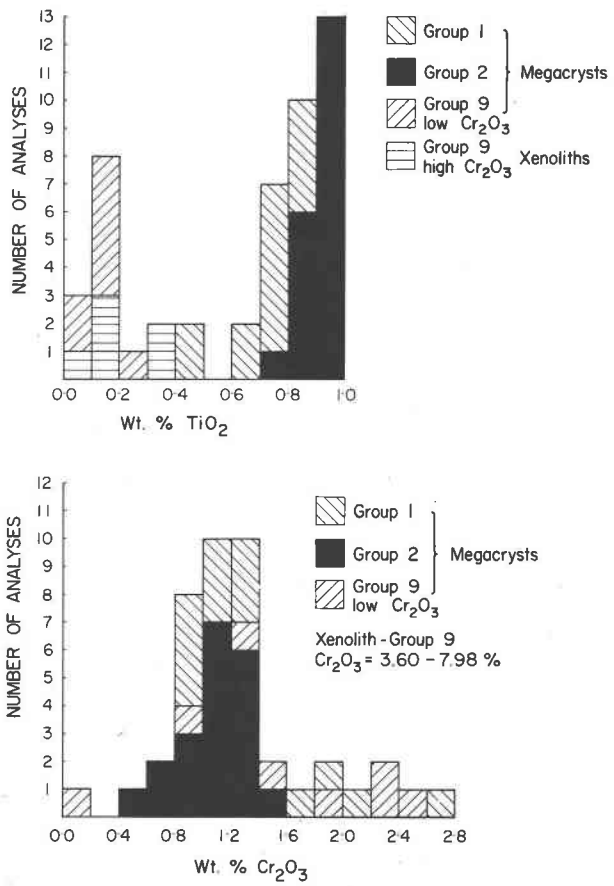

Fig. 3. Cr_2O_3 and TiO_2 contents of garnets in megacrysts and Elwin Bay lherzolite xenoliths.

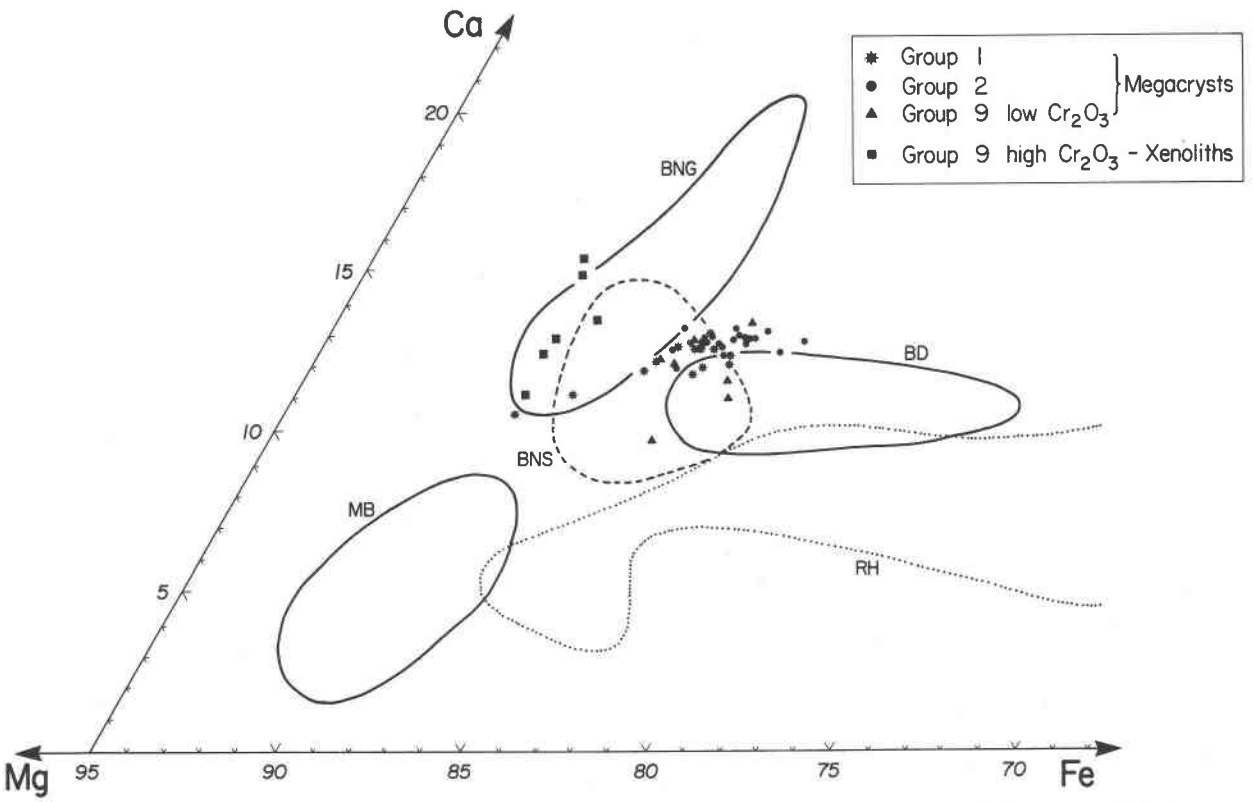

Fig. 4. Composition of garnets in Elwin Bay kimberlite and lherzolite xenoliths, compared with that of other mantle-derived garnets. MB, diamonds (Meyer and Boyd, 1972), BNG, BNS, granular and sheared lherzolites (Boyd and Nixon, 1975), BD, megacrysts from Frank Smith and Monastery (Boyd and Dawson, 1972), RH, megacrysts from kimberlite (Reid and Hanor, 1970).

(3) Opaque titaniferous-magnesian-aluminous-chromite that occurs only as a euhedral post-fluidization phase.

Representative analyses of the three types of spinel in this kimberlite are given in Table 4. Spinel compositions are plotted in Figure 5 as end-member spinel molecules in a reduced spinel prism (Mitchell and Clarke, 1976). This type of projection, in which total iron is calculated as FeO, is useful for kimberlite spinels which have probably formed under relatively reducing conditions, in that it includes all the major elements determined. The prism does not however indicate possible variations in Fe_3O_4 and $MgFe_2O_4$ content.

Aluminous-magnesian-chromite (AM-chromite) occurs as large (200μ) rounded transparent (reddish-orange) crystals which are compositionally uniform within individual grains. AM-chromites are characterized by low TiO_2(<1%) contents, and analyses therefore plot close to the base of the spinel prism. The spinels are similar in composition to AM-chromites in the Peuyuk kimberlite. Mitchell and Clarke (1976) have interpreted these chromites to be a series

Table 3. Composition of phlogopites from the Elwin Bay kimberlite; total Fe given as FeO

	1	2	3	4	5
SiO_2	40.95	41.45	35.07	35.37	34.80
TiO_2	0.57	1.29	4.24	0.75	0.65
Al_2O_3	12.44	12.38	14.95	17.90	16.92
Cr_2O_3	0.36	0.93	0.59	0.00	0.02
FeO*	3.43	3.05	4.27	2.57	2.23
MnO	0.04	0.06	0.05	0.04	0.05
MgO	24.45	26.55	23.41	23.97	23.44
CaO	0.03	0.02	0.05	0.10	0.03
Na_2O	0.34	0.09	0.27	0.04	0.64
K_2O	10.02	9.21	9.61	9.12	6.97
NiO	0.15	0.14	0.00	0.00	0.00
	92.79	95.15	92.17	88.84	85.15

1 - 3 phlogopite megacrysts.
4 - 5 chloritized groundmass phlogophite.

Table 4. Representative analyses of spinels from the Elwin Bay kimberlite

	1	2	3	4	5	6	7	8
TiO_2	0.10	0.27	0.88	2.17	5.38	3.05	4.09	6.57
Al_2O_3	13.94	12.27	11.49	2.40	1.66	9.98	8.70	10.07
Cr_2O_3	52.29	54.27	52.63	56.02	43.70	50.28	47.04	33.73
FeO*	18.79	19.61	20.67	26.27	39.70	21.00	25.86	31.04
MnO	0.41	0.38	0.37	0.44	0.48	0.45	0.47	0.53
MgO	13.93	13.48	13.07	11.56	8.53	14.95	13.66	16.81
	99.46	100.28	99.11	98.86	99.45	99.71	99.82	98.75
Recalculated Analyses (a)								
Fe_2O_3	6.89	6.84	7.25	11.29	17.71	8.75	11.08	19.76
FeO	12.58	13.86	14.15	16.11	23.77	13.12	15.89	13.26
	100.14	100.97	99.84	99.99	101.20	100.59	100.93	100.73
End Member Spinels. mol.%								
$MgAl_2O_4$	24.9	22.0	20.7	4.4	2.9	17.2	14.8	15.7
Mg_2TiO_4	0.3	0.9	3.0	7.6	17.7	10.1	13.3	19.6
$MnCr_2O_4$	1.1	0.9	1.0	1.2	1.2	1.1	1.2	1.2
$MgCr_2O_4$	37.7	37.9	34.9	38.8	10.6	34.6	26.2	24.2
$FeCr_2O_4$	24.1	26.4	27.9	24.5	38.5	22.5	26.4	9.7
Fe_3O_4	11.8	11.8	12.5	19.7	29.1	14.5	18.1	29.5

*Total Fe as FeO
(a) Recalculation by Carmichael's (1967) method.
1 - 3 aluminous magnesian chromite.
4 - 5 Al-poor titan-magnesian chromite.
6 - 8 titan-magnesian-aluminous chromite.

of high-pressure phenocrystal spinels formed in the mantle prior to fluidized intrusion of the kimberlite. The AM-chromites from Elwin Bay are typically mantled by opaque titaniferous spinels.

The least abundant spinel type is an Al_2O_3-poor titaniferous-magnesian-chromite (2–5% TiO_2; <3% Al_2O_3). This spinel occurs as mantles on AM-chromite, as rounded crystals mantled by more aluminous spinels, and as euhedral crystals. These spinels therefore appear to have been contemporaneous with fluidization and the immediate post-fluidization period.

The majority of euhedral groundmass spinels are titaniferous-magnesian-aluminous-chromites (titan-MA-chromite) with 3–7% TiO_2 and 6–10% Al_2O_3, which are continuously zoned towards titaniferous margins. These spinels form mantles around the earlier spinels and appear to have crystallized entirely after fluidization.

The titan-MA-chromites are themselves mantled by thin corroded and incomplete rims of spongy Ti-free magnetite intimately intergrown with minute crystals of perovskite and rutile.

Mantling relationships indicate that the spinel compositional trends are from AM-chromite to titaniferous-magnesian-chromite to titan-MA-chromite. This reflects an initial trend of increasing Fe/(Fe+Mg) and decreasing Al/(Al+Cr) ratios, followed by the reverse trend of increasing Al/(Al+Cr) and decreasing Fe/(Fe+Mg), to an approximately constant Fe/(Fe+Mg) ratio with increasing Ti content across the spinel prism, towards the magnesian ulvospinel–ulvospinel apex.

The compositional space occupied by the Elwin

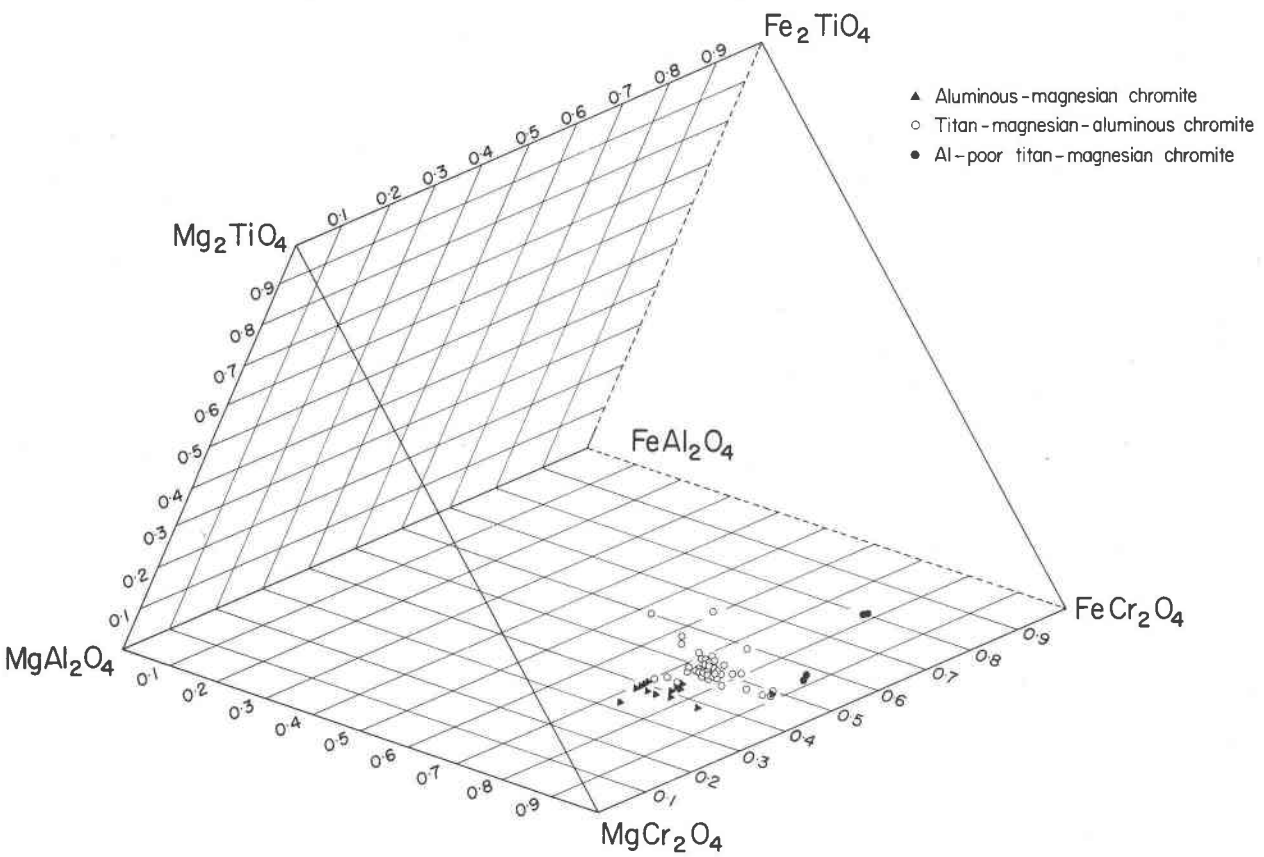

Fig. 5. Compositions of spinels plotted in a reduced spinel prism.

Bay spinels is compared with that of the Peuyuk spinels (Mitchell and Clarke, 1976) in Figure 6, which indicates that compositions and crystallization trends are identical. The Elwin Bay spinel assemblage is closest to that of Peuyuk B, except that TiO_2 enrichment is not as pronounced and the development of "atoll spinels" (Mitchell and Clarke, 1976) is rare. No members of the magnesian ulvospinel–ulvospinel–magnetite series appear to have formed at Elwin Bay.

Monticellite

Monticellite is present in variable quantities (up to 50% modally) in the groundmass, as euhedral colorless to pale yellow crystals. Monticellite has been considered to be a rare mineral in kimberlite, and relatively few positive identifications, *e.g.* Dawson (1962), have been made. Clement *et al.* (1975) have proposed that monticellite is in fact a common constituent of the groundmass; its apparent rarity may be due to lack of recognition and/or common alteration to carbonate. Clement *et al.* (1975) have found that monticellite is abundant in many South African kimberlites in which it was previously undiscovered. Representative analyses of monticellite are given in Table 5 and the compositional variation illustrated in Figure 7, which shows that the monticellites can contain up to 18 mol percent $CaFeSiO_4$ and 10 mol percent Mg_2SiO_4. Monticellites are zoned from iron-rich cores to iron-poor margins. Solid solution with Mg_2SiO_4 in these kimberlite monticellites is more extensive than that predicted by Warner and Luth's (1973) study of the iron-free Mg_2SiO_4–$CaMgSiO_4$ solvus. Monticellite together with phlogopite is also found at Elwin Bay in metasomatized limestone xenoliths.

Groundmass minerals

In addition to the above minerals, the principal groundmass minerals are perovskite, serpentine, calcite, pyrite, and apatite.

Perovskite occurs as rounded to euhedral crystals and is identical in composition (FeO = 1.2–1.7%) to perovskites found in other kimberlites (Mitchell, 1972). Thin discontinuous rims of rutile are devel-

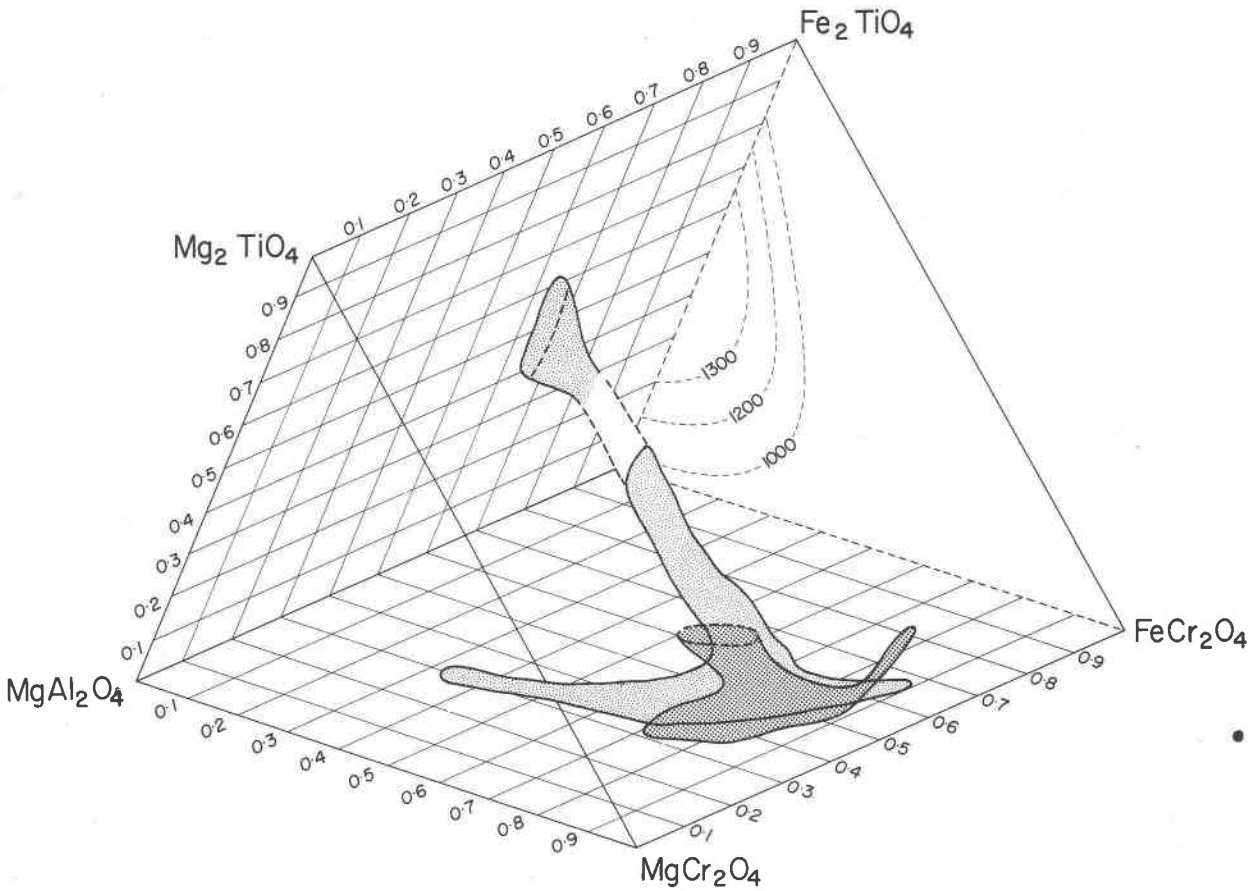

Fig. 6. Compositional field of spinels from Elwin Bay (dark stipple) and the Peuyuk kimberlite (light stipple) (Mitchell and Clarke, 1976).

oped around the perovskite. These rims are similar to those described by Mitchell and Clarke (1976) in the Peuyuk B kimberlite but are not as well developed. Apatite and pyrite occur as euhedral crystals scattered throughout the groundmass.

The major part of the groundmass, hereafter termed the silicate–carbonate groundmass, in which all the minerals described above are set, is an intimate mixture of very fine-grained serpentine and calcite. Calcite laths, commonly found in this groundmass, do not appear to be replacing an earlier mineral and therefore are considered to be primary.

Scattered throughout the silicate–carbonate groundmass are ocelli of calcite and serpentine. The common discontinuous veins and irregular patches of calcite in the kimberlite may represent coalescence of such ocelli. No oxides or silicates except serpentine are present in the ocelli.

The ocelli contain carbonates of two habits: (1) calcite rhombs lining the walls of the ocelli, while the remaining volume is filled by serpentine, and (2) acicular calcite crystals along the walls set in a matrix of serpentine, the center of the ocellus being a few rounded calcite crystals (Fig. 8). Carbonate in all habits is pure calcite, and no dolomite has been found. The serpentine is similar in composition to other serpentines in this kimberlite (Table 2, analyses 7 and 8).

Structures such as seen in Figure 8 could only have been formed after fluidization, and the ocelli may represent the separation of an immiscible carbonate liquid during the last stages of crystallization. The different habits of the calcite in the ocelli may represent different quenching rates. It should be particularly noted that *primary* serpentine crystallized from the late-stage carbonate-rich liquid. Primary serpentine has also been observed in carbonate-rich dikes at the Premier mine (Robinson, 1975) and in the groundmass of the Nigerdlikasik kimberlite (Andrews and Emeleus, 1971). By analogy much of the serpentine in the silicate–carbonate groundmass may also be primary.

Table 5. Representative partial analyses of monticellite from the Elwin Bay kimberlite

	1	2	3	4	5
SiO_2	37.50	36.83	36.65	36.84	36.64
FeO	3.09	3.73	5.67	6.41	7.47
MgO	24.71	24.09	24.11	23.07	22.50
CaO	34.77	34.06	33.06	32.04	32.11
	100.07	98.71	99.49	98.36	98.72
Mol. % end members					
$CaFeSiO_4$	6.8	8.3	12.5	14.5	16.3
$CaMgSiO_4$	90.9	88.4	80.6	78.2	75.9
Mg_2SiO_4	2.4	3.3	6.9	7.3	7.2

(Also present TiO_2, 0.02-0.10%; Al_2O_3, 0.15-0.25%; MnO, 0.22-0.41%.)

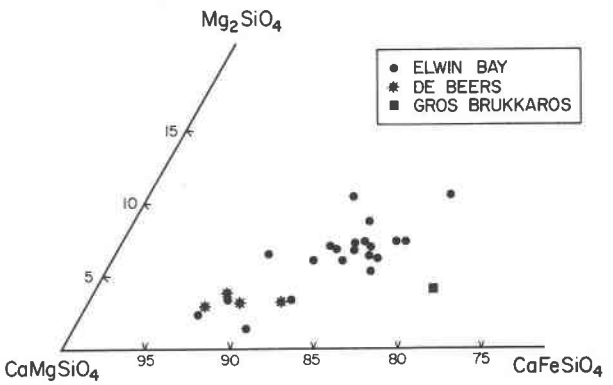

Fig. 7. Composition of monticellite expressed as molecular percentage of Mg_2SiO_4, $CaMgSiO_4$, and $CaFeSiO_4$. Data for De Beers kimberlite and Gros Brukkaros peridotite from Clement *et al.* (1975).

Crystallization history

The crystallization history of the kimberlite is outlined in Figure 9. Experimental (Wyllie and Huang, 1976) and geochemical (Mitchell and Brunfelt, 1975) studies indicate that kimberlite magmas are formed by partial melting of garnet lherzolite mantle. This magma initially crystallized pyrope and olivine. As the magma ascended towards the crust, pressure decreased and garnet ceased to be a liquidus phase; its place was taken by AM-chromite and by phlogopite in the later pre-fluidization crystallization history. The kimberlite was emplaced as a single fluidized intrusion, the fluidization resulted in the rounding of all pre-fluidization phenocrysts and ultramafic mantle-derived xenoliths. Post-fluidization crystallization resulted in the eventual development of late-stage volatile-rich fluids which separated as an immiscible carbonate fluid or formed carbothermal veins (Wyllie, 1966). Crystallization must have been relatively rapid in order that ocelli be preserved and that dense ultramafic xenoliths did not sink back into the magma conduit. The presence of the assemblage monticellite, calcite, and apatite indicates that temperatures were probably as low as 600°C during the crystallization of the groundmass (Wyllie, 1966). Franz and Wyllie (1967), for example, have found a eutectic in the system CaO–MgO–SiO_2–H_2O–CO_2 at 605°C involving portlandite, calcite, monticellite, and brucite. In kimberlites, portlandite and brucite may be represented by apatite and serpentine respectively. Textural evidence indicates that the calcite–serpentine ocelli crystallized in part after the silicate–carbonate groundmass, and therefore must have formed at even lower temperatures. Based upon spinel compositions, oxygen fugacities during immediate post-fluidization times were probably on the order of 10^{-19} to 10^{-21} bars (Mitchell and Clarke, 1976).

The Elwin Bay kimberlite presents in its crystallization sequence some similarities to that of Peuyuk B, but crystallization was arrested at Elwin Bay before extensive TiO_2 enrichment could occur and before the serpentine–carbonate immiscible liquid could inter-

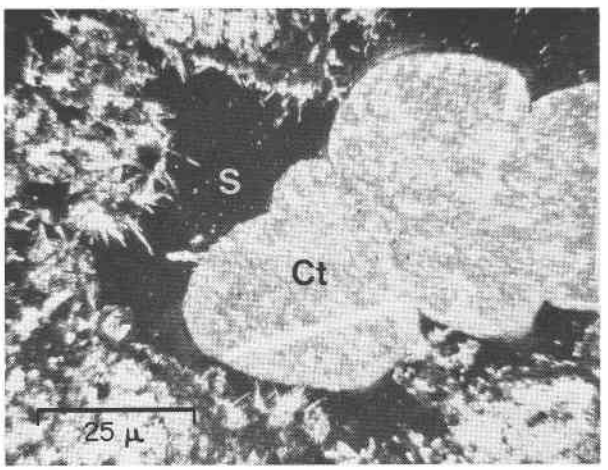

Fig. 8. Calcite (Ct)–serpentine (S) ocelli.

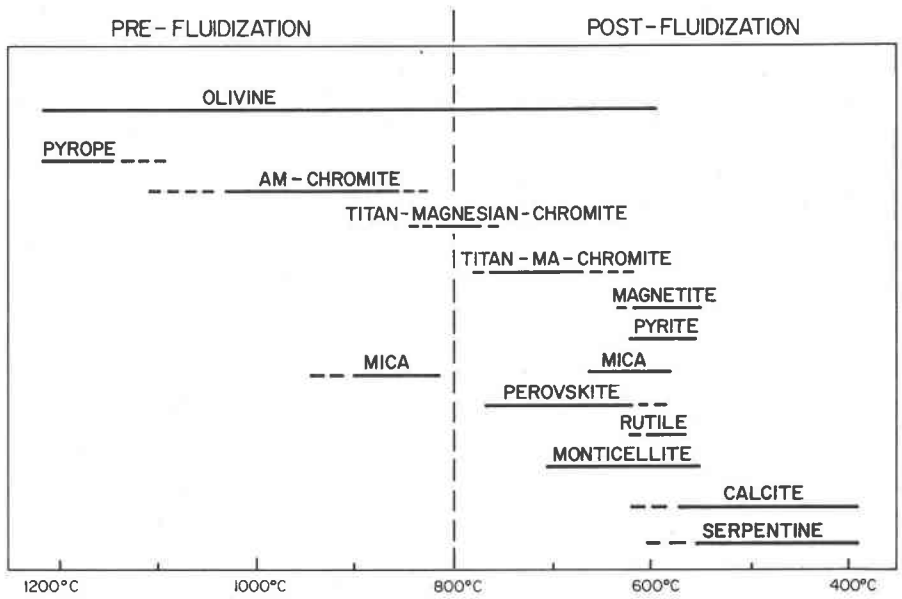

Fig. 9. Crystallization history of the Elwin Bay kimberlite. Temperatures are approximate only and are based upon data presented by Mitchell and Clarke (1976), Wyllie and Huang (1976), and Franz and Wyllie (1967).

act with the silicate–carbonate groundmass to any appreciable extent.

A characteristic feature of all the Somerset Island kimberlites so far examined in any detail (*e.g.* Peuyuk, Korvik-Selatiavak, and Elwin Bay) is the development of late-stage carbonate-rich fluids. This is in accord with experimental studies of synthetic kimberlites in the system CaO–MgO–SiO_2–H_2O–CO_2 by Wyllie and Huang (1976) and Franz and Wyllie (1967). It should be noted that these late-stage carbonates *are not* carbonatites of the type found associated with nepheline-bearing alkaline rocks, even though they are of primary magmatic origin, and that any petrogenetic hypotheses which attempt to link together kimberlitic and carbonatitic magmatism are ill-founded. This "kimberlite–carbonatite" relationship will be discussed in a subsequent paper. The carbonate-rich dikes and segregations associated with kimberlites at Somerset Island, the Benfontein sill (Dawson and Hawthorne, 1973), and the Premier mine (Robinson, 1975) should be referred to simply as carbonate dikes, and the associated carbonate-rich kimberlites should perhaps be termed calcareous kimberlites (Mitchell, 1970) rather than carbonatitic kimberlites.

Acknowledgments

This work is supported by the National Research Council of Canada. Henry Meyer is thanked for access to the Purdue University microprobe. The field work was undertaken as part of the Geological Survey of Canada's Project Boothia, and J. W. Kerr is thanked for much help and logistical assistance. The assistance and hospitality provided by personnel of Diapros Canada Ltd. is highly appreciated, and R. L. Davies and J. B. Hawkins in particular are thanked for their interest in this project. Marsha Mitchell is thanked for field assistance and collecting all the garnet megacrysts.

References

Andrews, J. R. and C. H. Emeleus (1971) Preliminary account of kimberlite intrusions from the Frederickshab district of southwest Greenland. *Geol. Surv. Greenland,* Rep. 31.

Bence, A. E. and A. L. Albee (1968). Empirical correction factors for electron microanalyses of silicates and oxides. *J. Geol., 76,* 382–403.

Boyd, F. R. and R. V. Danchin (1974) Discrete nodules from the Artur de Paiva kimberlite, Angola. *Carnegie Inst. Wash. Year Book, 73,* 278–282.

——— and J. B. Dawson (1972) Kimberlite garnets and pyroxene–ilmenite intergrowths. *Carnegie Inst. Wash. Year Book, 71,* 373–378.

——— and P. H. Nixon (1975) Origins of ultramafic nodules from some kimberlites of northern Lesotho and the Monastery mine. *Phys. Chem. Earth, 9,* 431–454.

Carmichael, I. S. E. (1967) The iron–titanium oxides of salic volcanic rocks and their associated ferromagnesian silicates. *Contrib. Mineral. Petrol., 14,* 36–74.

Clarke, D. B. and R. H. Mitchell (1975) Mineralogy and petrology of the Somerset Island kimberlite, N. W. T., Canada. *Phys. Chem. Earth, 9,* 123–135.

Clement, C. R., J. J. Gurney and E. M. W. Skinner (1975) Monticellite—an abundant groundmass mineral in some kimberlites. *Kimberlite Symposium, Cambridge, Extended Abstracts,* 71–73.

Dawson, J. B. (1962) Basutoland kimberlites. *Bull. Geol. Soc. Am., 73,* 545–560.

——— and J. B. Hawthorne (1973) Magmatic sedimentation and carbonatitic differentiation in kimberlite sills at Benfontein, South Africa. *Q. J. Geol. Soc. London, 129,* 61–85.

——— and J. V. Smith (1975) Chemistry and origin of phlogopite megacrysts in kimberlite. *Nature, 253,* 336–338.

——— and W. E. Stephens (1975) Statistical classification of garnets from kimberlite and associated xenoliths, *J. Geol., 83,* 589–607.

Eggler, D. H. and M. E. McCallum (1974) Xenoliths in diatremes of the western United States. *Carnegie Inst. Wash. Year Book, 73,* 254–300.

Emeleus, C. H. and J. R. Andrews (1975) Mineralogy and petrology of kimberlite dike and sheet intrusions and included peridotite xenoliths from south-west Greenland. *Phys. Chem. Earth, 9,* 179–197.

Finger, L. E. and C. Q. Hadidiacos (1972) Electron microprobe automation. *Carnegie Inst. Wash. Year Book, 71,* 598–600.

Franz, G. W. and P. J. Wyllie (1967) Experimental studies in the system CaO–MgO–SiO_2–CO_2–H_2O. In P. J. Wyllie, Ed., *Ultramafic and Related Rocks,* p. 323–326. John Wiley and Sons, New York.

Meyer, H. O. A. and F. R. Boyd (1972) Composition and origin of crystalline inclusions in natural diamonds. *Geochim. Cosmochim. Acta, 36,* 1255–1273.

Mitchell, R. H. (1970) Kimberlite and related rocks—a critical reappraisal. *J. Geol., 78,* 686–704.

——— (1972) Composition of perovskite in kimberlite. *Am. Mineral., 57,* 1748–1753.

——— (1976) Kimberlites of Somerset Island, District of Franklin. *Geol. Surv. Can. Pap., 76-1A,* 501–502.

——— (1977) Ultramafic xenoliths from the Elwin Bay kimberlite, the first Canadian paleogeotherm. *Can. J. Earth Sci., 14,* 1202–1210.

——— and A. O. Brunfelt (1975) Rare earth element geochemistry of kimberlite. *Phys. Chem. Earth, 9,* 671–686.

——— and D. B. Clarke (1976) Oxide and sulphide mineralogy of the Peuyuk kimberlite, Somerset Island, N. W. T. Canada. *Contrib. Mineral. Petrol., 56,* 157–172.

——— and P. Fritz (1973) Kimberlite from Somerset Island, District of Franklin, N. W. T. Canada. *Can. J. Earth Sci., 10,* 384–393.

Reid, A. M. and J. S. Hanor (1970) Pyrope in kimberlite. *Am. Mineral., 55,* 1374–1379.

Robinson, D. N. (1975) Magnetite-serpentine-calcite dykes at Premier Mine and aspects of their relationship to kimberlite and to carbonatite of alkalic carbonatite complexes. *Phys. Chem. Earth, 9,* 61–70.

Warner, R. D. and W. C. Luth (1973) Two-phase data for the join monticellite ($CaMgSiO_4$)–forsterite (Mg_2SiO_4): experimental results and numerical analysis. *Am. Mineral., 58,* 998–1008.

Wyllie, P. J. (1966) Experimental studies of the carbonatite problem: The origin and differentiation of carbonatite magmas. In O. F. Tuttle and J. Gittins, Eds. *Carbonatites,* p. 311–352. Interscience, New York.

——— and W. L. Huang (1976) Carbonation and melting reactions in the system CaO–MgO–SiO_2–CO_2 at mantle pressures with geophysical and petrological applications. *Contrib. Mineral. Petrol., 54,* 79–108.

Manuscript received, May 17, 1977; accepted for publication, August 23, 1977.